Electronic coupling between a FeSe monolayer film and $SrTiO_3$ substrate

Y. N. Huang[1,2,3] and W. E. Pickett[3,*]

[1]*Key Laboratory of Materials Physics, Institute of Solid State Physics, Chinese Academy of Sciences, P. O. Box 1129, Hefei 230031, China*

[2]*University of Science and Technology of China, Hefei, Anhui 230026, China*

[3]*Department of Physics, University of California Davis, Davis, California 95616, USA*

(Received 30 December 2016; revised manuscript received 4 March 2017; published 5 April 2017)

Several experimental groups have reported superconductivity in single unit cell layers of FeSe on $SrTiO_3$ and a few other substrates, with critical temperature T_c reports ranging up to 100 K, and a variety of theoretical work has been done. Here we examine more closely the interaction of a single FeSe layer with a TiO_2 terminated $SrTiO_3$(001) (STO) substrate. Several situations are analyzed: the underlying ideal interface, the effect of z-polarized longitudinal optic [LO($\hat{z}$)] phonons in STO, electron doping of the STO substrate, substitution of Se by the bordering chalcogenides S and Te, and doping by adsorption of K on the FeSe surface. These results complement earlier studies of O and Se vacancies. The O p_y, p_y surface band of STO persists at the interface, and by sharing holes with the hole pocket of FeSe it plays a part in the behavior around the interface, initially by determining the Fe Fermi level lineup with the STO band gap. The LO($\hat{z}$) mode causes strong band shifts around the interface but the strength of coupling to the Fe bands cannot be obtained with our methods. Adsorption of 25% K (one K per four Fe) fills the small O interface hole pocket and donates the rest of the electrons to the Fe hole pockets, filling them.

DOI: 10.1103/PhysRevB.95.165107

I. INTRODUCTION

The enhancement of the superconducting transition temperature T_c in FeSe, from 8 K in bulk [1] to 65 K or even 100 K when grown as single-unit-cell (1UC) layer on $SrTiO_3$ (STO) (we refer to this system as 1FeSeSTO) or related substrates [2–5], has generated intense interest because of suggestions that Cooper pairing can be strengthened by interface or substrate processes. Importantly, the anomalously large superconducting gaps are found in 1UC FeSe films but not in 2UC or thicker layers, making strict two dimensionality (2D) and strong quantum confinement central issues. Much of the focus is placed on the mechanism for enhanced pairing, and how and whether the interface may play a role in this enhanced superconductivity. A topical review has been provided by Wang *et al.* [6].

Angle resolved photoelectron emission spectroscopy (ARPES) spectra also have led to a probable role of interactions involving phonons at the interface, providing coupling that may enhance the energy scale of Cooper pairing and even change the pairing symmetry, thereby increasing the superconducting transition temperature T_c [7,8]. The specific observation implicating phonons was the detection of "replica bands" in ARPES spectra, in which secondary binding energy peaks ~100 meV toward higher binding energy were observed. STO itself has a flat optical phonon branch lying near 100 meV [9–11]. The suggestion has been that the replica bands are due to shake-off of quanta of longitudinal optical phonon modes in STO, reminiscent of the vibron shake-offs in the photoemission spectra of H_2 molecules [12]. This interpretation of the replica band requires strong coupling between FeSe carriers and substrate phonons. If such coupling is indeed strong, it would require including in the pairing interaction and might enhance T_c [13–15]. With the various scenarios that have been put forward, the pairing mechanism (or enhancement) in 1UC FeSe film remains uncertain.

Several studies of the electronic behavior of FeSe epitaxial films have been addressed with first-principles density functional theory methods, appropriate because properties seem to be very system dependent. Liu *et al.* found the Fermi level (E_F) of 1UC FeSe to shift into the STO band gap [7] with electron doping of STO (001). Unless otherwise noted, all studies assume TiO_2 termination of the STO substrate. Considerable charge transfer from the STO substrate to 1UC FeSe was obtained by Zheng *et al.* [16], giving rise to an intrinsic electric field in the interfacial region. Bazhirov *et al.* suggested that charge doping in FeSe leading to an increase in the density of states at E_F, $N(E_F)$, may be the important factor [17].

Anion vacancies (O and Se) require consideration, since they can serve as the source of electron doping as found by Bang *et al.* [18] although Linscheid found that large vacancy concentration is required for significant charge transfer [19]. Charge transfer from oxygen vacancies to the 1UC FeSe layer was also found by Cao *et al.* to suppress the magnetic order there, potentially promoting enhanced superconductivity [20]. Shanavas and Singh (SS) found that both O vacancies in the STO substrate and excess Fe over the monolayer can provide high levels of electron doping [21]. A somewhat different viewpoint arises from evidence that doped electrons accumulated at the interface were presented by Liu *et al.* [22]. Se vacancies were considered by Berlijn *et al.* [23], who observed unanticipated character of anion vacancies, behaving more as hole donors than electron donors.

The possible role of phonon-enhanced pairing has attracted substantial interest. Coh *et al.* suggested that AFM characteristics of 1UC FeSe may open important electron-phonon coupling channels [24]. Liu *et al.*, who observed that their FeSe+STO samples contained only Γ-centered electron pockets, suggested the simpler Fermi surfaces suggested a different pairing mechanism [25]. Using a 1.5% compressively

*wepickett@ucdavis.edu

strained STO substrate, the first-principles calculations of Li *et al.* obtained an enhancement of electron-phonon coupling compared to bulk FeSe, but must be too small to explain the observed T_c, from which they concluded lattice coupling could not justify the observed high T_c [26].

The broad and varied picture just presented has been complemented by experimental reports [27,28] that T_c can reach 46 K in films of FeSe due to electron doping by K adsorption, in which doping is suspected to be limited to the first layer or two of FeSe. This range of T_c is the same as obtained on K-doped bulk FeSe, from which Wen *et al.* [27] suggest the interface (and by implication the substrate) does not play any significant role in the enhancement of superconductivity. From the evolution of the Fe bands upon increasing K doping (up to ∼25%), from dispersive to flat to incoherent as seen by ARPES, they suggest a strong change in interelectronic correlation effects must be considered. Miyata *et al.* [28] also found that K doping of FeSe films on STO could increase T_c up to the same range of critical temperatures, including inducing high T_c beginning from a nonsuperconducting 1FeSeSTO sample. The increase in superconducting gap with decrease in the thickness of the FeSe thin film led them to conclude that some interfacial (or substrate) effects are crucial. Seo *et al.* [29] studied alkali metal adsorption on a few UC layers of FeSe deposited on bulk FeSe (with T_c no higher than 8 K). The critical temperate was raised to 20 K, and their analysis of ARPES data suggested that only the surface layer of FeSe was doped, and therefore the interface was not playing a role in this enhancement of T_c.

While the influence of the substrate on FeSe remains very uncertain, a common expectation is that oxygen vacancies are required to explain the filling of the Γ-centered hole pockets as observed in ARPES studies. The needed concentration of surface layer vacancies is of the order of 10%, and modeling them even in a simple periodic manner leads to supercells that would be computationally expensive as well as challenging to interpret (viz. several inequivalent Fe and Se sites and a profusion of bands). With 10% vacancies there may well be ∼2 nm^2 regions where the TiO_2 surface layer of STO is intact. For such regions, their underlying interfacial electronic structure needs to be understood.

In this paper first-principles methods, described in Sec. II, are applied to probe several basic features of the electronic structure of 1FeSeSTO for stoichiometric STO, and then consider a number of situations that are relevant to various experimental data on this system. In Sec. III we present the basic underlying electronic structure and bonding of the static structure, and then investigate the effect of frozen longitudinal optic phonons in the STO substrate. Electronic doping of the substrate is investigated in Sec. IV. In Sec. V atomic substitutions for Se and adsorption of K on FeSe are analyzed. A discussion and synopsis follows in Sec. VI.

II. STRUCTURE AND METHODS

A. Structure of the simulation cell

To study the 1FeSeSTO system, we choose a symmetric TiO_2 terminated slab, 2.5 unit cells thick along the c axis, separated by a vacuum layer. The 1UC FeSe is added to the top of the slab as shown in Fig. 1. The surface-to-monolayer distance is defined as the separation along c axis between Fe and Ti planes, $d_S = z_{Fe} - z_{Ti} = 4.19$ Å and $d_X = z_{Se} - z_{Ti} = 2.91$ Å. Distances were chosen from among those studied by SS [21], as discussed below. The tetragonal cell has lattice constants $a = 3.905$ Å, $c = 23.28$ Å.

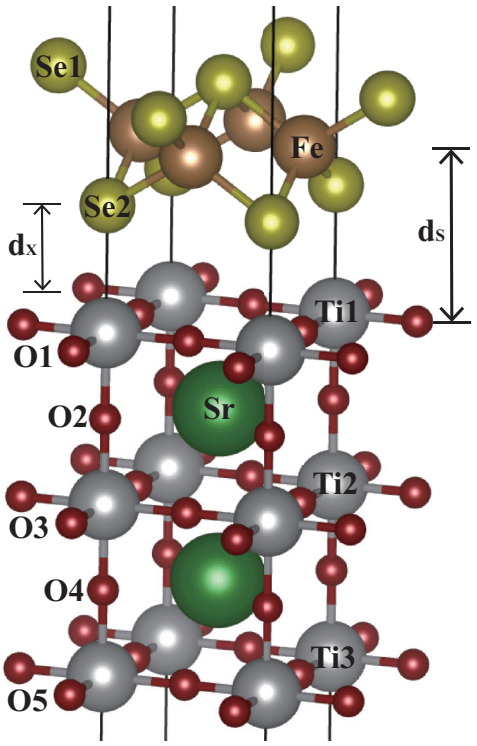

FIG. 1. The structure of the simulation cell of 1 unit cell of FeSe on a $SrTiO_3$ substrate, with site designations as used in this paper. The marked interlayer distances are defined as $d_S = z_{Fe} - z_{Ti}$ and $d_X = z_{Se} - z_{Ti}$, where z_i are the z coordinate of the atom.

Frozen phonon calculations for the in-plane $Q = 0$ longitudinal optic [LO($\hat{x}$)] and $\hat{z}$-axis polarized LO($\hat{z}$) mode were carried out for 1FeSeSTO. The model phonon displacements and other details are provided in Sec. III B.

Since coupling between FeSe and the STO substrate is broadly anticipated to underlie the enhanced superconductivity in this system, the distance between overlayer and substrate is a crucial parameter to understand. Presuming (based on bulk FeSe) that FeSe provides a charge-neutral 1UC overlayer, the van der Waals (vdW) interaction may play a significant role in the interlayer bonding. Liu *et al.* [22] reported that the distance between the top Se atom of the first unit cell and the TiO_2 termination plane of the substrate is about 5.56 Å when accounting for the vdW interaction, which would be consistent with the reported experimental value 5.5 Å [2]. With this value, $d_S = 2.66$ Å. However, SS [21] gave evidence to support d_S lying between 4.19 and 4.44 Å, while also accounting for the vdW interaction between 1UC FeSe and TiO_2 surface layer.

B. Computational methods

The full-potential linearized augmented plane wave Wien2K package [30] has been used for the electronic structure calculations. We use the Perdew, Burke, and Ernzerhof (PBE)

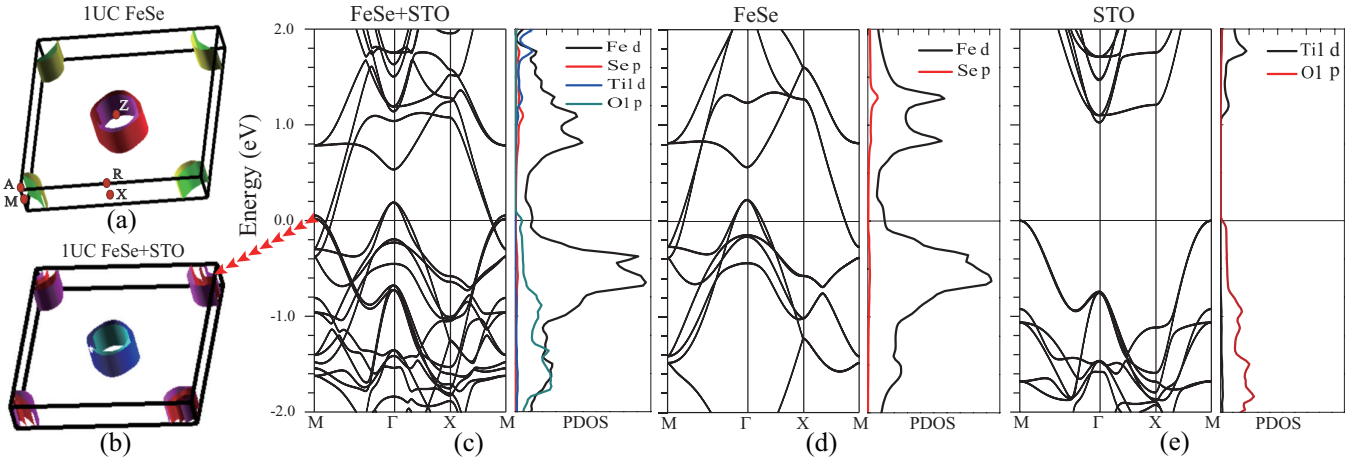

FIG. 2. Calculated Fermi surfaces of (a) 1UC FeSe and (b) 1FeSeSTO, the difference is at the corner M point. The electronic band structures and projected densities of states (pDOS) are shown for (c) 1FeSeSTO, (d) 1UC FeSe, and (e) STO. The valence band maximum of STO has been aligned with the two Fermi levels in (c) and (d), which is very near where the STO bands lie in (c). The bands of 1FeSeSTO are simply a overlay of those of the two parts, reflecting only how they align across the interface. The red arrows indicate the Fermi surfaces arising from the O1 interface band.

[31] version of the generalized gradient approximation (GGA) within density functional theory. The sphere radii for Fe, Se, Ti, O, and Sr are taken as 2.25, 2.14, 1.93, 1.74, 2.20, and 2.50 bohrs, respectively. The basis set cut-off parameter $R_{mt}K_{\max} = 7.0$ was found to be sufficient. The number of **k** points was ∼4500 for the tetragonal unit cell that was used for each of the calculations to provide adequate sampling of small Fermi surfaces.

The distance between FeSe and the surface TiO_2 layer has been much discussed but not settled. To assess the effect of this separation, we have carried out studies at three Se-Ti distances $d_s = 4.11$, 4.19, and 4.44 Å, with the corresponding band structures shown in the Supplemental Material [32]. We have used in our calculations the 4.19 Å separation preferred by SS [21].

Lee [14] proposed to model the sandwich with 1UC FeSe on both sides of the STO slab, thinking that the phonon mediated interaction will be modeled better in that configuration than in a polar simulation cell. To test the underlying differences of using a symmetric (nonpolar) cell versus STO covered on only one edge (as in experiment), we calculated the electronic structure for 2.5UC STO with 1UC FeSe on both surfaces. One difference was that the oxygen surface/interface band in TiO_2 (discussed extensively below) is filled in the symmetric cell, while it provides a small fraction of holes in the 1FeSeSTO structure. As noted above, we have used the asymmetric simulation cell pictures in Fig. 1.

III. ANALYSIS AND INTERPRETATION

A. Coupling of FeSe to STO

Several aspects of the electronic structure of this system were noted briefly in the Introduction, and we build on them. Growth of FeSe on STO(001) may result in charge transfer depending on the band lineup (Schottky barrier), hence some doping of the FeSe layer with respect to bulk FeSe. We first study this possibility and quantify the effect.

Figure 2 shows the band structure of 1FeSeSTO, and those of the isolated subsystems FeSe and STO, along with the Fermi surfaces (FSs) of the first two. The STO slab is terminated by two TiO_2 surfaces, a termination that is widely used as a substrate for film growth with one surface covered with 1UC FeSe. Bulk STO is a 3.2 eV direct gap (at Γ) insulator, which becomes around 2 eV in GGA calculations due to the well known underestimation of the gap in DFT calculations. Since only the valence band is involved in processes near the Fermi level in FeSe, the underestimate of the STO gap does not have any serious impact.

The right-hand panel of Fig. 2 reveals an indirect (M-Γ) gap of only 1 eV. The upper valence band at M is a well known feature of the (001) surface of STO (and $BaTiO_3$), arising from p_x, p_y orbitals [33] on the surface layer O ion whose on-site energy is raised by the lack of an adjoining SrO layer. The O-O hopping path is between nearest neighbors which lie along (110) directions, hence the rather large dispersion of ∼1.5 eV is only along Γ-M, not along Γ-X. There are actually two of these bands, one from each surface, but they are essentially degenerate, indicating the lack of coupling of the STO surfaces through the insulating "bulk" of two unit cells.

This STO surface band assumes importance because its maximum slightly overlaps the Fermi level of FeSe, thereby pinning the lineup of Fe d bands and the STO band gap. We note that in the calculations of Li and co-workers [26] with 1.5% compressively strained STO as the substrate, this surface band did not reach the Fe Fermi level, thus the relatively band edges may be sensitive to such strains. We used the unrelaxed, experimental lattice constant for STO because that conforms to the experimental situation.

Single layer FeSe displays the common feature of several Fe-based pnictides and chalcogenides as this band filling: two hole surfaces at Γ, and two electron surfaces at M. In the combined 1FeSeSTO system, the bands are practically a simple overlap of the STO and the FeSe bands. This does not mean there is no coupling between STO and FeSe, but rather

that the interface O1 p_x, p_y orbitals are uncoupled to the Fe d orbitals except by charge transfer.

As pointed out by SS [21], the Fermi level of 1FeSeSTO lies 1 eV above the STO valence band maximum, i.e., roughly in the middle of the STO gap. Thus even with stronger coupling across the interface, states at E_F would decay quickly into STO, again supporting the use of a rather thin STO layer. A feature not previously pointed out is that the O1 surface (interface) band at M pins E_F: if the Fe Fermi level were to lie lower than the surface band at M, charge would flow from the surface O states to Fe states, raising E_F until the Fe Fermi level and the interface O Fermi levels coincide. In fact, our result is that this does occur to a slight extent (50 meV overlap), the small hole FSs at M are shown in Fig. 2, lying inside the Fe FSs at M. Note also that the two surface bands (one now an interface band) remain practically degenerate. The amount and character of charge transferred will be quantified below. The important qualitative result is that the Fermi level of FeSe is pinned by the STO interface band maximum.

The projected densities of states (pDOS) also reflect minor influence of the electronic coupling between STO and FeSe: $N(E_F) = 1.64$ eV^{-1} per Fe and 1.69 eV^{-1} per Fe atom in 1FeSeSTO and FeSe, respectively. The small band overlap results in $N(E_F) = 0.66$ eV^{-1} on the interface O ion, an appreciable amount due to the steplike DOS of two-dimensional bands.

Now we turn to the charge density ρ of the three systems. 1FeSeSTO is the one of interest, which we compare with the sum of that of an isolated slab of 1UC FeSe and of an isolated slab of STO(001). These calculations were carried out in identical unit cells to facilitate the comparison in terms of the difference density

$$\Delta\rho = \rho_{\text{1FeSeSTO}} - [\rho_{\text{FeSe}} + \rho_{\text{STO}}]. \quad (1)$$

This difference density provides the "rearrangement" of charge due to the interaction (bonding or repulsion) of FeSe and STO, including of course the fact that two surfaces become one interface.

Figure 3 presents a color plot of the difference density in the (110) plane that contains an Fe-Se2-Fe chain and what is normally thought of as a (100) plane of STO containing TiO_4 units. Positive values designate regions where charge increases when the coupling of FeSe and STO is incorporated. The changes are rather small, consistent with the neutral and nonpolar nature of both isolated systems, but involve orbital repopulation in the FeSe layer and on the interface Ti ion. In the interior of STO there is some breathing of ionic charge on both Ti and O, reflecting some long range effect due to the insulating nature of STO. There is some (anisotropic) loss of charge from the interface O ion, consistent with the slight band overlap and resulting hole pocket discussed above. The most important change is the strongly anisotropic rearrangement of density on Fe: d_{xz},d_{yx} regions have decreased density, while in-plane (d_{xy}) regions increase in density. The interface Se2 atom also shows an anisotropic response to coupling, which can be characterized best as the development of some Se2-Ti1 bonding. Dumitrescu *et al.* have studied a model adapted to 1UC FeSe in which the interaction favors breaking of equal occupation of d_{xz} and d_{yx} orbitals, and find that doping indeed introduces a superconducting phase [34].

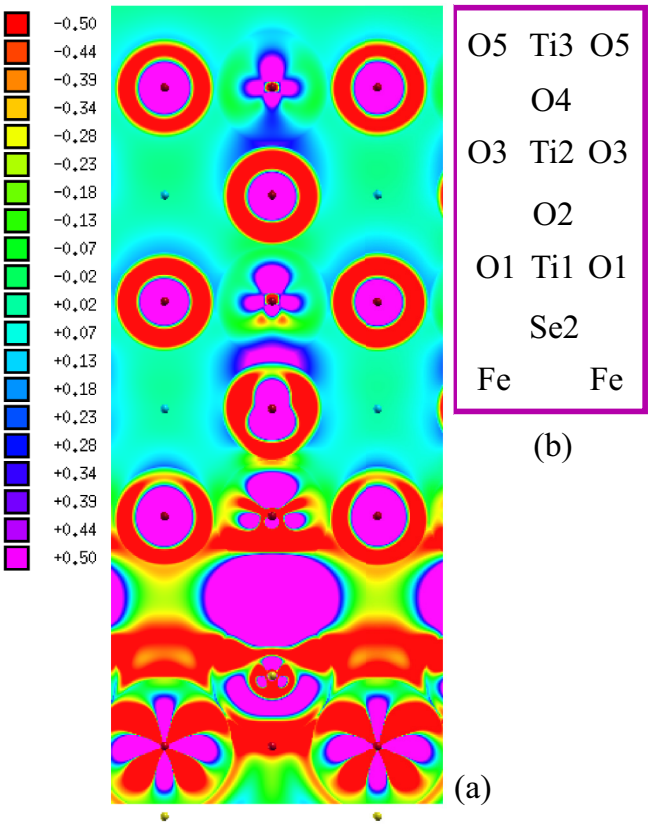

FIG. 3. (a) Color plot of the difference density FeSeSTO − (FeSe + STO), in 10^{-3} atomic units, with FeSe lying at the bottom. The color scale is at the left. (b) Atomic positions in the (110) plane shown in (a). The surface Se atom does not lie in this plane. The differences are rather small (see text) but the rearrangement of charge on the Re atom at the bottom is evident.

B. Electron-LO phonon coupling

Observation of replica (or shadow) bands in ARPES studies of 1FeSeSTO and 1UC FeSe on TiO_2, with energy shift equal to the LO mode of the substrate, has spurred study of a phonon-enhanced mechanism of pairing, notwithstanding the most prominent viewpoint that the most likely mechanism of bulk pairing in Fe-based superconductors is magnetic in origin. As a complementary technique, high resolution electron energy loss spectroscopy has been applied by Zhang *et al.*, who found strong coupling of a surface optical mode of STO to the conduction electrons [35]. To get an idea of the character and strength of coupling of optic modes in STO to the Fe d band Fermi surface states in 1FeSeSTO, we have performed calculations of the FeSeSTO system with model frozen phonons in the STO substrate. Displacements of 0.10 Å for O, and −0.05 Å for Ti and Sr, were chosen as being approximations to the maximum displacement of these ions in an optic mode. (Using harmonic oscillator expressions with an energy of 100 meV, the maximum O displacement, $\sqrt{2}$ times the r.m.s displacement in the $n = 1$ oscillator mode, is 0.088 Å, which we have rounded up.) Making the LO($\hat{z}$) displacements in the x-y plane, which directs the internal electric field also in the x-y plane, very small changes in FeSe were found. This outcome is consistent with two observations:

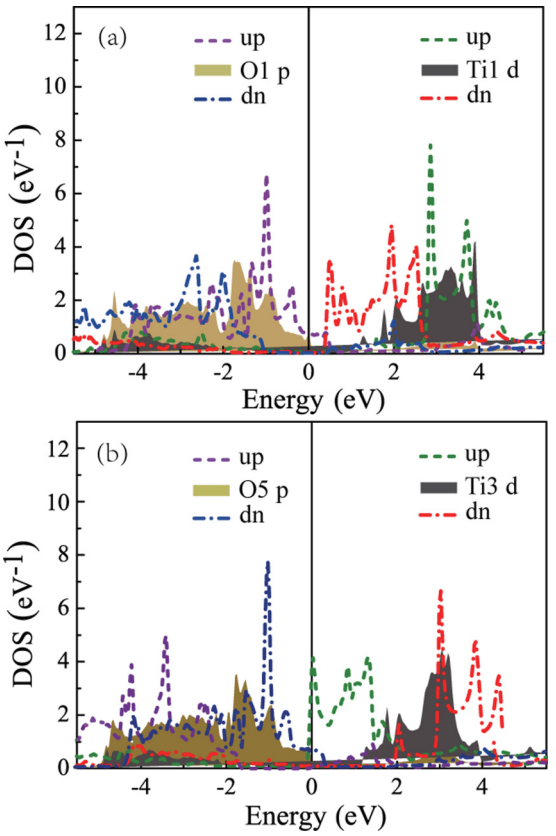

FIG. 4. Atom projected densities of states (pDOS) of (a) the interface Ti1 and O1 ions, and (b) the bottom surface Ti3 and O5 ions of 1FeSeSTO in z-polarized LO mode. "up" refers to O ions moving toward the FeSe layer and cations moving oppositely; "dn" refers to displacement in the opposite direction. The pDOS for the undisplaced (reference) position are filled in.

(1) the electric field in such a displacement would be directed parallel to, and not into, the FeSe layer, and (2) the single unit cell periodicity imposed in the x-y plane does not allow in an internal electric field, that is, a true LO mode with its accompanying polarization is not replicated in such a periodic cell.

LO($\hat{z}$) mode displacement, however, leads to large effects. To describe the changes, oxygen displacement toward the FeSe layer will be called positive (or up), the opposite will be called negative (or dn). The displacements are large enough that the changes (in bands, DOS, and density) are not equal in size but opposite in sign, instead they contain nonlinear changes that may be useful to consider. The atom-projected pDOS are provided in Fig. 4, and the corresponding band structures in Fig. 5, for positive, zero, and negative displacements.

The pDOS provides one broad view of relative shifts in STO due to the LO mode, with energy zero pinned at the Fe Fermi level. At the interface, the peak in the O1 p DOS shifts by roughly ± 1 eV, but we will see below that certain band shifts are unexpected. The Ti1 d bands shift sharply for dn movement, while shifting upward mildly for up displacement. The electric field in the STO reverses from up to dn displacement, and the band shifts on the free surface O5 and Ti3 atoms are roughly opposite to those at the interface.

For surveying the bands, the items to focus on are (i) the filling of Fe hole (Γ) and electron (M) pockets, (ii) the position of the Ti d bands, and (iii) the position of the O1 surface (interface) band with its maximum at M. Regarding the Fe band fillings, the up displacement increases the hole filling while decreasing the electrons in their pocket. The changes are opposite in sign for the dn displacement. The Fermi level (the energy reference for the different calculations) is pinned in the Fe d bands, which therefore are affected in ways that are more involved to quantify. The STO bands are shifted substantially by the internal electric field.

While the FSs centered at M are very similar for up and dn displacements (not shown, but readily imaginable from Fig. 5), they are different from those for the undisplaced configuration: the interface or surface O1 p_x, p_y band (depending on direction of displacement) discussed above moves well above E_F, by 0.25–0.35 eV. The resulting holes require that electrons are driven into the Fe d bands. These electrons are accommodated mostly in the M-centered pockets; the number of holes around Γ varies somewhat.

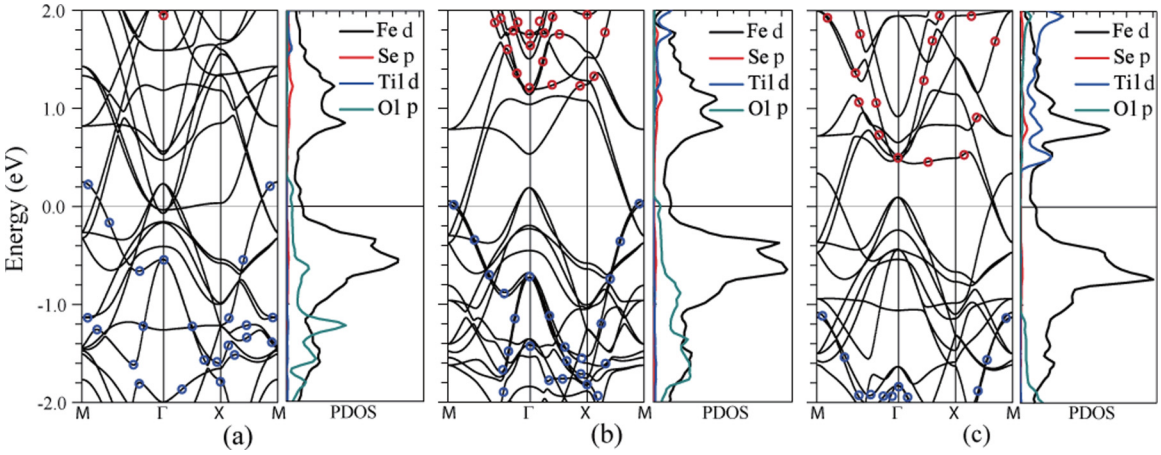

FIG. 5. Band structures for the frozen LO($\hat{z}$) phonon: (a) up, (b) reference undisplaced, and (c) dn displacements, see text. Red circles indicate strong Ti1 character, while blue circles represent strong O1 character of the band. In all cases the Fermi level is pinned by the Fe d bands, but some changes are nonmonotonic (viz. the O p bands).

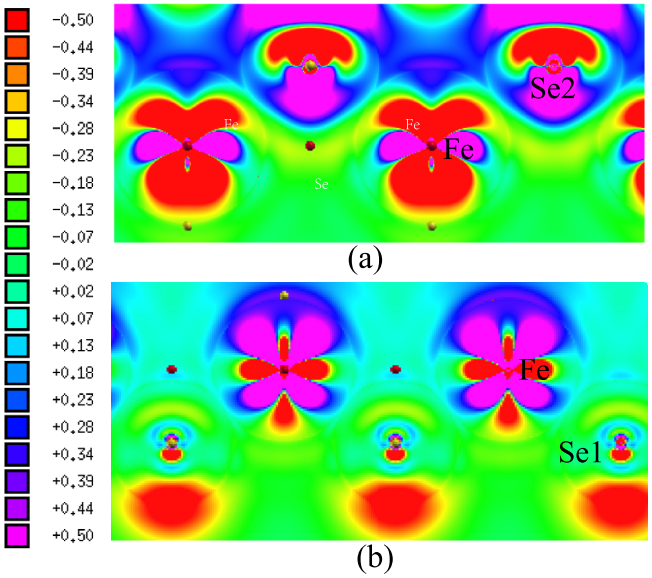

FIG. 6. Difference density (in 10^{-3} a.u.) in 101 plane containing (a) the Fe-Se2-Fe chain, and (b) the Se1-Fe-Se1 chain. For the orbital re-occupation on Fe, see text.

The behavior of several bands at Γ is unexpected. The top of the STO valence band at Γ (marked by blue circles) rises mildly for the up displacement but drops by 1 eV for dn displacement. Ti3 p bands at the free surface (without any circles in the figure) drop to E_F for up displacement, from being out of the picture for dn displacement. A related shift at Γ is: for negative displacement Ti1 valence d bands drop from ∼2 eV for the up displacement, to 1.2 eV for undisplaced, to within 0.5 eV of E_F. This energy is the STO conduction band minimum at the interface Ti1 ion. More information is provided in the Supplemental Material [32].

The difference density

$$\Delta\rho = \rho(\text{1FeSeSTO}) - \rho[\text{LO}(\hat{z})] \quad (2)$$

due to the mode displacements is shown in Fig. 6 in two planes containing Fe. Positive values designate regions where downward displacement of O in the mode increases the density. In the Fe-Se2-Fe chain direction for positive displacement, Fig. 6(b), the occupation of Fe in-plane orbitals is decreased, while in Fe-Se1-Fe chain plane, Fig. 6(a), the electron occupation of the Fe in-plane orbitals is increased. For positive displacement the orbital occupation differences for Fe inside the atomic spheres are, in 10^{-3} units,

$$[d_{z^2}, d_{x^2-y^2}, d_{xy}, d_{xz}, d_{yz}] : [-2.0, 2.9, 0.8, -11.0, 11.6]. \quad (3)$$

The net change here is a $+2.3 \times 10^3$ electrons, or 0.023 e/Å oxygen displacement, increase. For negative displacement, again in units of 10^{-3}, the orbital occupation differences for Fe are

$$[d_{z^2}, d_{x^2-y^2}, d_{xy}, d_{xz}, d_{yz}] : [10.4; -15.7; 4.2; 16.6, -20]. \quad (4)$$

The net change is -4.5×10^{-3} electrons, an increase of 0.045 holes/Å, holes. Note that the net change in each case is a factor of 3–5 smaller than some of the orbital occupations, reflecting the strong reoccupation of Fe d orbitals with much smaller net change in charge.

The differences in magnitudes of these differences reflect the nonlinear nature of the 0.1 Å displacement. A more interesting, and perhaps more important, aspect is the just mentioned, relatively larger re-occupations. They are large for d_{xz}, d_{yz} orbitals for both directions of displacement, and for negative displacement also large for $d_{z^2}, d_{x^2-y^2}$ orbitals.

IV. EFFECTS OF SUBSTRATE DOPING

Doping of the STO substrate is of interest for at least two reasons. First, STO used as substrates may be naturally doped, or they can be intentionally doped to facilitate measurements that might be affected by charging of the STO interface. Second, intentional doping of FeSe can be used to study the effect on the FeSe overlayer and perhaps even to tune its properties, especially if gating is applied. For these reasons we have studied the effects of electron doping by STO of the FeSe layer. Electron doping of bulk STO results in superconductivity below a maximum of 0.4 K in a certain range of light doping levels [36]. Hole doping of STO, as might occur at this interface, has not been reported to result in itinerant carriers in bulk STO.

Virtual crystal doping in $SrTiO_3$

The observation that electron carriers in STO readily become itinerant even at very low doping levels indicates that a realistic means of studying electron doping is to use the virtual crystal approximation (VCA). In VCA, the charge on a nucleus is increased or decreased in an amount equal to the density of carriers one wants to simulate. VCA is appropriate for itinerant states in alloys, because extended wave functions average over many ions. Since STO is commonly electron doped by substitution of Nb^{5+} for Ti^{4+}, the VCA models substitution of a fraction x replacement of Ti with Nb by an increase in the Ti nuclear charge from 22 to $22 + x$. A simpler rigid band treatment would simply dump x extra electrons per Ti into the conduction bands without any change of the band structure, thus they would reside in the Fe 3d bands (with a few filling the O1 interface hole band). VCA includes the self-consistent rearrangement of electronic charge, allowing charge to reside anywhere in the system including transfer of doped electrons to the FeSe layer and, crucially, the self-consistent adjustment of the Fermi energy in STO with that in FeSe. What VCA cannot do is to treat specific local doping effects, such as might occur at the immediate interface. However, physical values of dopants in STO are of the order of 10^{-4}/unit cell or less, making the dopants rather sparse at the interface.

The simplest picture of the effect of STO doping is the following. Recall that before doping, E_F as determined by filling of Fe levels lies roughly in the middle of the STO band gap, as described above. Doping electrons into the bands puts them, before self-consistency, into the Fe 3d bands just above E_F and also fills holes in the O 2p interface band, none of them residing within the STO substrate. The charged substrate will provide an attractive potential tending to attract carriers back into STO. Only self-consistency can determine the outcome. However, the complete system is characterized

by a single chemical potential, so Fermi levels in FeSe and bulk STO must coincide. A simplistic realignment of the two Fermi levels, assuming some carriers are retained in STO, requires a relative shift of potential in FeSe and STO of the order of 1 eV or more, even for much lighter doping levels than we consider. Such a shift requires substantial energetic changes, and what is expected is that charge will rearrange between STO and FeSe to minimize the total energy of the system as the Fermi levels are equalized.

At small electron doping, the tendency to align Fermi levels will drive electrons doped into Ti $3d$ bands toward and into FeSe, moving its Fermi level up toward the Ti Fermi level. From the well known behavior in doped semiconductors, electron density will accumulate in the interfacing region, leading to upward band bending within the Ti $3d$ bands. The result, if a mesoscopic picture of band bending were to apply, is a Schottky barrier across which the Fermi levels in Fe and STO equalize. Additional doping will lower the Schottky barrier (a region of positive potential between the equalized FeSe and STO Fermi levels) but it will persist.

Adequate sampling of resulting small FSs in STO requires us to model higher dopings than would be considered experimentally. (Perhaps effects of high doping in STO on the superconductivity in FeSe should be considered experimentally.) We have doped using the VCA method $x = 0.05$ and 0.10 electrons per Ti, which we expect to provide instructive results. The corresponding important band energies at Γ and M versus x are displayed in Fig. 7.

Certain primary features are evident. The Fe hole pockets at Γ and electron pockets at M provide a sink for carriers that leads to significant changes in net charge (electrons minus holes) in Fe. At 5% doping some electrons are transferred to Fe: the Γ-centered hole bands have fewer carriers, with more electrons around M. One change to note is that the STO interface O1 $2p$ hole band at M shifts downward rapidly with increasing x, becoming filled at much smaller x than we consider. The O3 and O5 levels shift downward even more quickly, although they are always filled. The overriding effects are that doped electrons reduce the density of Fe hole carriers, and the O1 $2p$ hole bands become completely filled. The most relevant accompanying shift is that the Ti $3d$ bands at Γ shift downward in energy substantially. For Ti2 and Ti3, the shift is -0.8 eV at $x = 0.05$ and -1.2 eV at $x = 0.10$. The "bulk" Ti2 band becomes occupied at $x = 0.10$; very roughly, this can be interpreted as the Fe and Ti Fermi levels becoming equalized at the second layer of Ti in STO—the Schottky barrier is a single unit cell thick. The interface Ti1 band remains unoccupied, as it provides the Schottky barrier of about 0.6 eV.

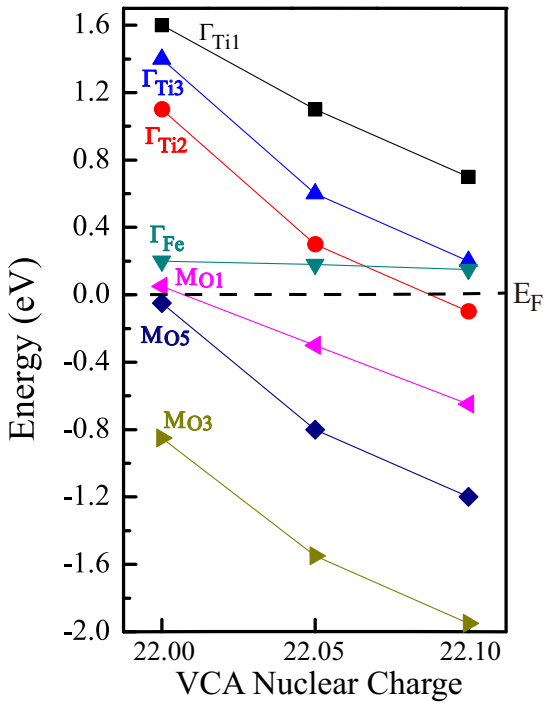

FIG. 7. Bands edges for Fe and Ti bands at Γ point, and O bands at the M point, for VCA nuclear charge equal to 22.00, 22.05, and 22.10.

Another means to assess the charge arrangement is to compare atomic sphere electronic charges versus x. About 70% of the doped-in charge resides within the inscribed spheres of Ti, O, and Fe, with the remaining charge in the tails of the orbitals outside the spheres. We simply scale up the total sphere charges to 100% for our overview. The specific values are provided in the Supplemental Material [32].

First, there is negligible change in charge on the Se atoms, and the changes are relatively small on the O atoms. In fact, in spite of the substantial changes in the energy position of O $2p$ and Ti $3d$ relative to the valence band maximum of Fe (which is always 0.15–0.20 eV above the Fermi level, this band effectively pinning E_F) seen in Fig. 7, much of the charge remains on the Ti sites. For oxygen, the change in charge for O1 is negligible, for O2 a change of electronic charge of -0.007 (a loss of electrons), and for O3, -0.012 ($x = 0.05$) to -0.015 (for $x = 0.10$), the changes not being linear. The changes are roughly the same for Ti1, Ti2, and Ti3 ions, a gain of 0.04 for $x = 0.05$, and ∼0.10 for $x = 0.10$. Hence Ti retains most of the doped charge although O ↔ Fe energy rearrangement does occur.

Fe obtains an increase in electrons as expected, but in a nonmonotonic fashion. The increase is 0.025 for $x = 0.05$ (with $3 \times 0.05 = 0.15$ extra electrons in the unit cell), and more than half of this increase can be said to come from O3 and O5 rather than from Ti ions. For $x = 0.10$, the increase for Fe drops to 0.20, again with a similar decrease in charge for O3 and O5. Only the three Ti ions show a roughly linear increase in electronic charge with doping, as they retain most of the doped-in charge. The rather small charge transfer to Fe but large energy shifts relative to Fe suggest that charge polarization effects are substantial in this system and might lead to Fe d band—STO lattice coupling.

V. ATOMIC SUBSTITUTIONS AND ADSORPTION

A. Isovalent chalcogenide substitution

Tendencies toward charge transfer and rearrangement can be probed by atomic substitutions, even isovalent ones. Isostructural Fe chalcogenides include FeS [37–40] and FeTe [39–41]. To make comparisons we focus on orbital occupations and charge density when Se is replaced with 50% S and Te,

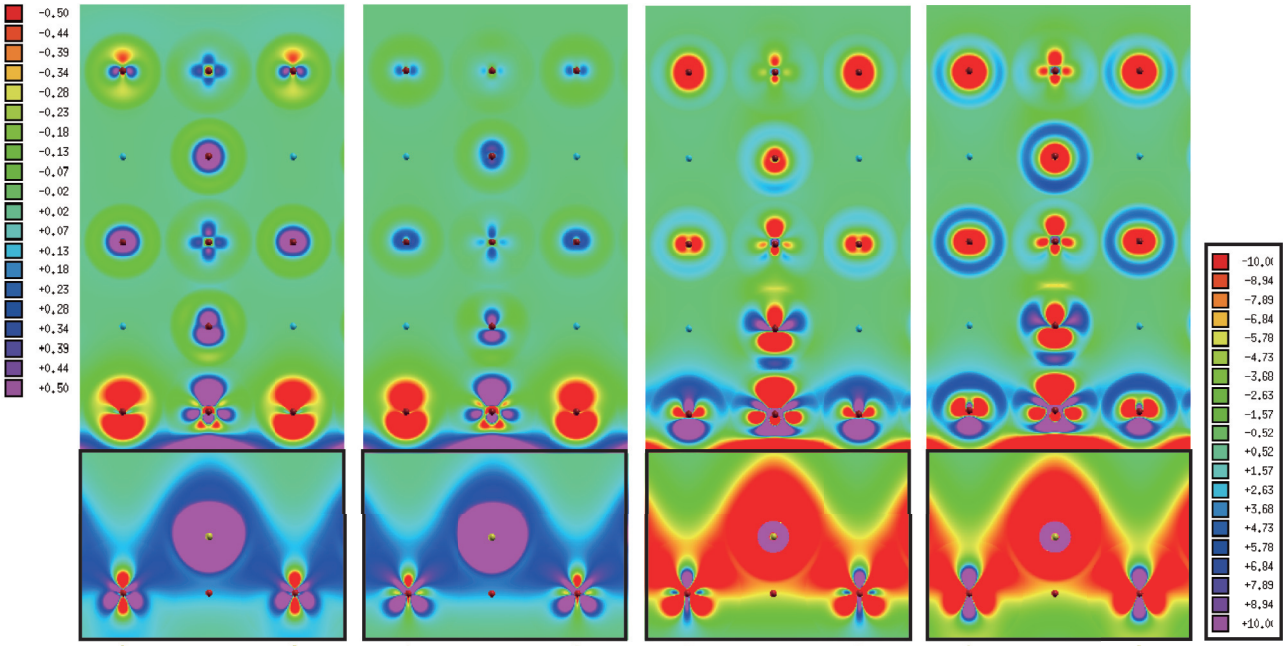

FIG. 8. Difference density, in 10^{-3} a.u., of ρ(1FeSeSTO) minus cells with Se replaced by a fraction x of S or Te, $x = 0.5$ and 1.0, as noted. The horizontal black separating line denotes where the color scale has been changed, because the differences are so much larger in the lower subpanels. Left color scale on the left is for upper subpanels, the one on the right is for the lower subpanels containing the Fe-X chain.

and also compare with the corresponding FeS and FeTe cases. These comparisons are referenced to the 1FeSeSTO structure and sample a range of chemical, electronegativity, and size differences.

There has been much attention focused on Fe orbital occupations and how they relate to properties, especially pairing. In Fig. 8 we display the difference charge density of these systems compared to ρ(1FeSeSTO). In the $FeS_{0.5}Se_{0.5}$ and $FeTe_{0.5}Se_{0.5}$ "alloys" an S or Te layer replaces the Se layer nearest STO, that is, at the interface, entailing no change in symmetry of the system. Since FeX (X = S, Se, Te) is a metal, even isovalent substitution may result in some charge transfer between Fe and the chalcogenide, or the STO substrate as well, so the substitution might somewhat dope the Fe layer.

Figure 8 shows color plots, ordered monotonically in terms of average normalized electropositivity of the chalcogenide atoms, of difference densities in a (101) plane containing an interface Fe-Se chain, and the designated atoms in the STO layers. Relaxation is not included, since as noted above changes due to even small displacements would mask changes in difference plots due solely due to chemical differences. Positive values designate regions where Se attracts charge relative to S or Te.

Figures 8(a) and 8(b) for S replacement, and likewise Figs. 8(c) and 8(d) for Te replacement, reveal similar trends for the half and full Se replacement cases. The main difference is that full replacement of Se leads to differences that extend further into the STO layer. The effect on orbital (re)occupation on Fe is almost independent of half versus full replacement of S. Likewise, the differences in the TiO_2 interface layer is almost independent of fraction of replacement. This result seems reasonable, since in each case the replacement has occurred in the Se2 layer at the interface.

On the other hand, there are noteworthy differences between substitution by S and by Te. The changes in orbital occupations on Fe (i.e., the shapes of the differences) are rather similar but opposite in sign, with the same being true of Ti1 at the interface. The change on O1 is different: for S substitution the change is all in the p_z orbital, while for Te substitution the reoccupation involves all $3p$ orbitals.

To quantify and summarize differences for the various substitutions we have studied, Fig. 9 illustrates graphically the (ir)regularities in the variation of Fe $3d$ orbital occupations (which are small), and the net change of $3d$ charge is shown in Fig. 9(b). The d_{xy}, d_{z^2}, and $d_{x^2-y^2}$ occupations vary nearly linearly across the entire range, with the first two increasing, and the latter decreasing, from S to Te. The d_{xz} and d_{yz} occupations vary nonlinearly and in an opposing manner. The regularity of the net change in d charge, in Fig. 9(b), indicates that there is charge redistribution between these two orbitals for the $x = 0.5$ concentrations of S-Se and Se-Te. The lack of equivalence of these two orbitals is due, first to the asymmetry around Fe for the $x = 0.5$ concentrations, and from the basic simulation cell, in which Fe lies above an O1 ions that has Ti neighbors along only one of the x, y axes.

B. Adsorption K on FeSe

Doping of single layer FeSe on STO by K adsorption has resulted in superconductivity up to 46 K. To assess the electron donation from K to FeSe+STO we have added one K in the center of a surface Se1 square in a $\sqrt{2} \times \sqrt{2}$ enlargement of the cell, corresponding to 25% K doping (i.e., one K per four

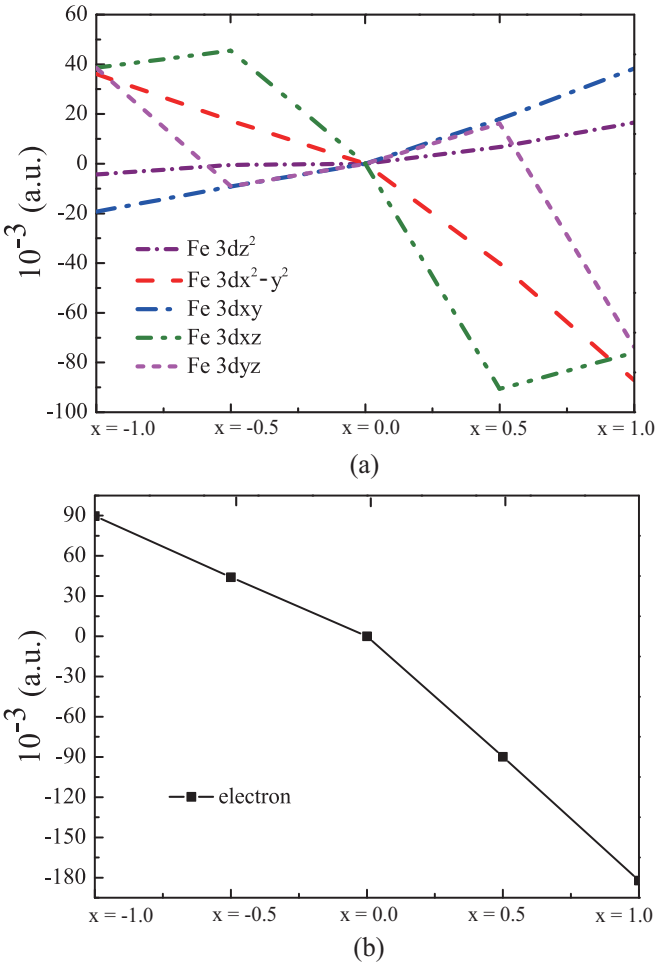

FIG. 9. (a) Orbital occupation differences, in 10^{-3}, versus a normalized mean electropositivity difference x, supposing $x = -1$ for S, 0 for Se, and +1 for Te, and (b) the net change of charge in all Fe d orbitals. The nonlinearities are discussed in the text.

Fe). For reference below, we note the relative x-y positions of K, Fe, and Se atoms in the $\sqrt{2} \times \sqrt{2}$ cell: K at (0.25,0.25); site Fe1 at (0.25,0.25); two Fe2 at (0.25,0.75) and (0.75,0.25); Fe3 at (0.75,0.75); two surface Se1 atoms at (0,0 and (0.5,0.5); two interface Se2 at (0.5,0) and (0,0.5). The K height was optimized, assuming a position 2.56 Å above the Fe layer. For analyzing the rearrangement of the density, the original atomic positions have been used in order to separate changes due to K addition from changes due to relative Fe-Se and Se-O displacements (which would cause large but uninteresting structure in the plots). The detailed results are unexpected in some respects.

The changes in band structure, displayed in Fig. 9 where bands have been backfolded due to the $\sqrt{2} \times \sqrt{2}$ in-plane doubling of the cell, and band filling are consistent with expectations of simple electron transfer from K to the bands near E_F. The hole bands to be filled are Fe d bands and the O p_x, p_y interface and/or surface bands. 25% doping is just the amount needed to do this, as can be seen in Fig. 10, and it leaves only Fe electron FS pockets such as has been seen on superconducting 1FeSeSTO (without intentional electron doping). The maximum of the interface O band remains

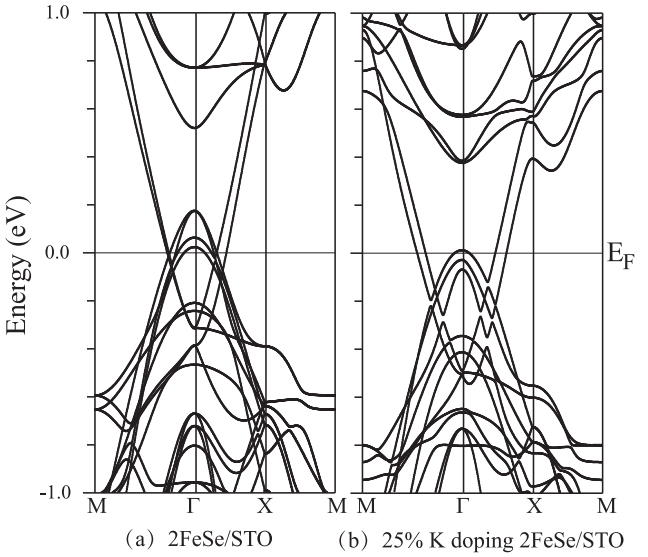

FIG. 10. Bands of (a) 1FeSeSTO and (b) for a 25% K overlayer 1FeSeSTO. The Fermi level (set to zero in each figure) increases by 0.2 eV, just enough to fill the hole bands at Γ.

touching E_F, while the back surface O band maximum lies 0.3 eV lower. This difference is consistent with the interface O1 ion being much closer to the added charge, thus lying at higher potential.

The change in charge density is more involved, and at first seems unphysical. The charge transferred to Fe1 lying directly below K is around 0.05 e, whereas there is no increase in charge for Fe2 and Fe3. The remainder of the charge is transferred to the nearby Se1 atoms, 0.10 e each. There is no net charge transferred to either O or Ti ions, though there is some minor rearrangement of occupations. This result is unexpected, since the hole pocket of the interface O p_x, p_y band is filled. This analysis of actual charge reflects the fact that occupied valence bands have shifts in spectral weight of orbital on Fe, Si, and O throughout the valence region that involve net charge change on only some of the atoms. The physical charge of K remains in its vicinity, on the neighboring Se1 and Fe1 atoms, however the hole bands are filled as if the charge went to the O1 ion and all Fe ions (not just Fe1).

Such counterintuitive rearrangements of charge have been discussed several times in the literature. One example is in recent studies of charge-ordering (CO) transition metal oxides. The most heavily studied example is the CO behavior in nickelates, for example $YNiO_3$. In the low temperature phase the CO characterization $YNi^{2+}_{1/2}Ni^{4+}_{1/2}O_3$ makes sense from the band (projected DOS) viewpoint: one Ni ion has strong spectral weight near the gap in two more bands than does the other Ni ion; the "d^8" ions are magnetic, roughly consistent with spin $S = 1$, the "d^6" ion has $S = 0$. Study of the actual charge density reveals that both Ni ions have the same occupation of 3d physical charge (same radial density) [42,43]. The difference lies in the distance to the coordinating O ions and the degree of spin polarization. Returning to this K doping case, the picture of filling of Fe d bands and O p interface bands is appropriate in that it is these bands that ARPES experiments

will probe. The changes in hybridization, and finally the actual charge, on various atoms may influence ARPES intensities.

VI. DISCUSSION AND SUMMARY

We have performed a first-principles study of several scenarios relating to experimental observations of the single unit cell of FeSe on STO, providing analysis that should assist the community in evaluating microscopic processed underlying observations. At the FeSe-STO separation determined by Shanavas and Singh [21], the FeSe Fermi level lies 0.7 eV above the bottom of the STO gap. However, the high lying surface band of O p_x, p_y orbitals on the $TiO_2(001)$ surface persists at the interface and contains holes, pinning the placement of the FeSe Fermi level within the STO band gap. The FeSe Fermiology is almost unaffected, with the d bands retaining both electron and hole pockets consistent with previous DFT studies. Comparison of 1FeSeSTO with the isolated subsystems shows a minor amount of charge transfer from the interface O1 ion to FeSe, and a small change in orbital occupations on Fe.

A frozen STO longitudinal optic phonon polarized in-plane has negligible effect on the FeSe electronic structure (although the accompanying electric field is not treated in our periodic simulation cell). For $\hat{z}$ polarization, the phonon causes large relative band shifts between those in STO and the FeSe bands. For the displacements studied, $+0.1$ Å for O, -0.05 Å for Ti, the relative band shifts of Ti d and Fe d orbitals approaches 2 eV, suggesting that polarizability provided by the unoccupied Ti d states may play a role in coupling. The resulting changes in the Fe orbital occupations have been quantified. For the magnitude of displacements we have studied (given just above), there are strong nonlinear aspects to orbital occupations and relative bands shifts of Ti and O with respect to those of Fe.

The results suggest strong coupling of the LO modes to the Fe d bands although no quantification such as electron-phonon matrix elements has been obtained. Rademaker *et al.* [15], following related work by Kulić and Dolgov [44] for cuprates, have studied the effect of an optic mode for Q at or near zero, coupled to a two-dimensional electronic system. In their model, confinement of the phonon Q to small values alters the behavior of $T_c(\lambda)$ at small coupling λ from the BCS exponential behavior to linear, making T_c more responsive to changes in coupling strength. Inclusion of Coulomb repulsion however has a similar effect. They did demonstrate that phonon-induced replica bands did appear in the resulting electronic spectral function.

Electron doping in STO was studied within the virtual crystal approximation, which presumes the electrons are itinerant, which is an excellent viewpoint in bulk STO where superconductivity appears at very low doping. 5% and 10% electron doping (viz. by Nb^{5+}) has been studied, the large value chosen to enable well-converged calculations which could not be achieved at the more realistic 0.1% or less level. Also, for lower doping levels the band bending in STO would extend to much longer distances in STO, which are not realistic to attempt with our methods. As anticipated for electrons doped into the STO conduction bands above the Fe Fermi level, some charge is transferred to the Fe d bands to align the strong band bending in STO and equilibrate the Fermi level in STO with that of Fe. The strong lowering of O1 p and Ti1 d levels at Γ and M were quantified.

For substitution in the chalcogenide column, Se at the interface was replaced by S and by Te (50% and 100% in the layer) with fixed positions, to assess the differences due to chemistry (electronegativities) and size of the chalcogenides. 100% replacement gives similar character of changes at the interface, but the effects extend further into STO than for 50%. The effect of S, versus Te, as the replacement atom showed up as clear differences on the Fe site, but also on both the O1 and Ti1 sites at the interface. This difference suggests that further experimental study of such substitutions could determine which is more favorable for superconductivity, and thereby what changes in the electronic structure are more favorable for pairing.

Finally, the experimental observation that adsorption of K onto (nonsuperconducting) 1FeSeSTO induces superconductivity has been studied by incorporation of 25% K adsorption (one K per four Fe atoms), using a $\sqrt{2} \times \sqrt{2}$ supercell. The effect is as anticipated: the electrons transfer to the hole bands of Fe and also of the O p_x, p_y surface/interface band. 25% just fills both bands leaving only the electron Fermi surfaces in FeSe. Analysis of the location of charge is revealing: the donated electrons from K reside nearby in adjoining Se and Fe atoms. The distribution of spectral density throughout the valence bands is affected, with the net physical results that hole pockets are filled as expected.

The mechanism of increased superconducting critical temperature observed in several cases of 1UC FeSe on various substrates is emerging as a complex question of several competing effects: doping, by unintentional oxygen vacancies, Fe-Se nonstiochiometry, or alkali atom adsorption; electron-phonon coupling induced by optic phonons in the underlying substrate; of indirect effects on the magnetic fluctuations in FeSe. We take no position at this time on the mechanism(s) that enhance T_c greatly relative to the 8 K value of bulk FeSe. Our various results impact most of the proposed models of mechanisms [3,6,8,13–16,24,26]. The latter possibility (indirect effect on magnetic fluctuations) has not been addressed in this work. The results we have presented for the effects of (i) $\hat{z}$-polarized optic modes in $SrTiO_3$, (ii) electronic doping in $SrTiO_3$, (iii) substitutional isovalent atoms for Se, and (iv) electron doping of the FeSe layer by K, should be of use in evaluating the complex behavior occurring at and near this interface.

ACKNOWLEDGMENTS

Calculations were performed at the Center for Computational Science of CASHIPS, the SciGrid of Supercomputing Center Network Information Center of the Chinese Academy of Science, and resources of the National Energy Research Scientific Computing Center, a DOE Office of Science User Facility supported by the Office of Science of the US Department of Energy under Contract No. DE-AC02-05CH11231. Y.H. was supported by the China Scholarship Council. W.E.P. was supported by National Science Foundation Award No. DMR 1607139.

[1] F. C. Hsu, J. Y. Luo, K. W. Yeh, T. K. Chen, T. W. Huang, P. M. Wu, Y. C. Lee, Y. L. Huang, Y. Y. Chu, D. C. Yan, and M. K. Wu, Superconductivity in the PbO-type structure α-FeSe, Proc. Natl Acad. Sci. USA **105**, 14262 (2008).

[2] Q. Y. Wang, Z. Li, W. H. Zhang, Z. C. Zhang, J. S. Zhang, W. Li, H. Ding, Y. B. Ou, P. Deng, K. Chang, J. Wen, C. L. Song, K. He, J. F. Jia, S. H. Ji, Y. Y. Wang, L. L. Wang, X. Chen, X. C. Ma, and Q. K. Xue, Interface-induced high-temperature superconductivity in single unit-cell FeSe films on $SrTiO_3$, Chin. Phys. Lett. **29**, 037402 (2012).

[3] D. Liu, W. Zhang, D. Mou, J. He, Y. B. Ou, Q. Y. Wang, Z. Li, L. Wang, L. Zhao, S. He, Y. Peng, X. Liu, C. Chen, L. Yu, G. Liu, X. Dong, J. Zhang, C. Chen, Z. Xu, J. Hu, X. Chen, X. Ma, Q. Xue, and X. J. Zhou, Electronic origin of high-temperature superconductivity in single-layer FeSe superconductor, Nat. Commun. **3**, 931 (2012).

[4] S. L. He, J. F. He, W. H. Zhang, L. Zhao, D. F. Liu, X. Liu, D. X. Mou, Y. B. Ou, Q. Y. Wang, Z. Li, L. L. Wang, Y. Y. Peng, Y. Liu, C. Y. Chen, L. Yu, G. D. Liu, X. L. Dong, J. Zhang, C. T. Chen, Z. Y. Xu, X. Chen, X. C. Ma, Q. K. Xue, and X. J. Zhou, Phase diagram and electronic indication of high-temperature superconductivity at 65 K in single-layer FeSe films, Nat. Mater. **12**, 605 (2013).

[5] S. Tan, Y. Zhang, M. Xia, Z. R. Ye, F. Chen, X. Xie, R. Peng, D. F. Xu, Q. Fan, H. C. Xu, J. Jiang, T. Zhang, X. C. Lai, T. Xiang, J. P. Hu, B. P. Xie, and D. L. Feng, Interface-induced superconductivity and strain-dependent spin density waves in $FeSe/SrTiO_3$ thin films, Nat. Mater. **12**, 634 (2013).

[6] L. Wang, X. Ma, and Q.-K. Xue, Interface high-temperature superconductivity, Supercond. Sci. Technol. **29**, 123001 (2016).

[7] K. Liu, Z. Y. Lu, and T. Xiang, Atomic and electronic structures of FeSe monolayer and bilayer thin films on $SrTiO_3$ (001): First-principles study, Phys. Rev. B **85**, 235123 (2012).

[8] Y. Y. Xiang, F. Wang, D. Wang, Q. H. Wang, and D. H. Lee, High-temperature superconductivity at the $FeSe/SrTiO_3$ interface, Phys. Rev. B **86**, 134508 (2012).

[9] N. Choudhury, E. J. Walter, A. I. Kolesnikov, and C. K. Loong, Large phonon band gap in $SrTiO_3$ and the vibrational signatures of ferroelectricity in $ATiO_3$ perovskites: First-principles lattice dynamics and inelastic neutron scattering, Phys. Rev. B **77**, 134111 (2008).

[10] C. Lasota, C. Z. Wang, R. Yu, and H. Krakauer, *Ab initio* linear response study of $SrTiO_3$, Ferroelectrics **194**, 109 (1997).

[11] W. G. Stirling, Neutron inelastic scattering study of the lattice dynamics of strontium titanate: Harmonic models, J. Phys. C **5**, 2711 (1972).

[12] D. W. Turner, Molecular photoelectron spectroscopy, Philos. Trans. R. Soc. London Sect. A. **268**, 7 (1970).

[13] J. J. Lee, F. T. Schmitt, R. G. Moore, S. Johnston, Y. T. Cui, W. Li, M. Yi, Z. K. Liu, M. Hashimoto, Y. Zhang, D. H. Lu, T. P. Devereaux, D. H. Lee, and Z. X. Shen, Interfacial mode coupling as the origin of the enhancement of T_c in FeSe films on $SrTiO_3$, Nature (London) **515**, 245 (2014).

[14] D. H. Lee, What makes the T_c of $FeSe/SrTiO_3$ so high?, Chin. Phys. B **24**, 117405 (2015).

[15] L. Rademaker, Y. Wang, T. Berlijn, and S. Johnston, Enhanced superconductivity due to forward scattering in FeSe thin films on $SrTiO_3$ substrates, New J. Phys. **18**, 022001 (2016).

[16] F. Zheng, Z. Wang, W. Kang, and P. Zhang, Antiferromagnetic FeSe monolayer on $SrTiO_3$: The charge doping and electric field effects, Sci. Rep. **3**, 2213 (2013).

[17] T. Bazhirov and M. L. Cohen, Effects of charge doping and constrained magnetization on the electronic structure of an FeSe monolayer, J. Phys.: Condens. Matter **25**, 105506 (2013).

[18] J. Bang, Z. Li, Y. Y. Sun, A. Samanta, Y. Y. Zhang, W. Zhang, L. Wang, X. Chen, X. Ma, Q. K. Xue, and S. B. Zhang, Atomic and electronic structures of single-layer FeSe on $SrTiO_3$(001): The role of oxygen deficiency, Phys. Rev. B **87**, 220503(R) (2013).

[19] A. Linscheid, Electronic properties of the FeSe/STO interface from first-principles calculations, Supercond. Sci. Technology **29**, 104005 (2016).

[20] H. Y. Cao, S. Y. Tan, H. J. Xiang, D. L. Feng, and X. G. Gong, Interfacial effects on the spin density wave in $FeSe/SrTiO_3$ thin films, Phys. Rev. B **89**, 014501 (2014).

[21] K. V. Shanavas and D. J. Singh, Doping $SrTiO_3$ supported FeSe by excess atoms and oxygen vacancies, Phys. Rev. B **92**, 035144 (2015).

[22] K. Liu, B. J. Zhang, and Z. Y. Lu, First-principles study of magnetic frustration in FeSe epitaxial films on $SrTiO_3$, Phys. Rev. B **91**, 045107 (2015).

[23] T. Berlijn, H. P. Cheng, P. J. Hirschfeld, and W. Ku, Doping effects of Se vacancies in monolayer FeSe, Phys. Rev. B **89**, 020501(R) (2014); H.-Y. Cao, S. Chen, H. Xiang, and X.-G. Gong, Antiferromagnetic ground state with pair-checkerboard order in FeSe, *ibid.* **91**, 020504 (2015).

[24] S. Coh, M. L. Cohen, and S. G. Louie, Large electron-phonon interactions from FeSe phonons in a monolayer, New J. Phys. **17**, 073027 (2015).

[25] K. Liu, M. Gao, Z. Y. Lu, and T. Xiang, First-principles study of FeSe epitaxial films on $SrTiO_3$, Chin. Phys. B **24**, 117420 (2015).

[26] B. Li, Z. W. Xing, G. Q. Huang, and D. Y. Xing, Electron-phonon coupling enhanced by the $FeSe/SrTiO_3$ interface, J. Appl. Phys. **115**, 193907 (2014).

[27] C. H. P. Wen, H. C. Xu, C. Chen, Z. C. Huang, X. Lou, Y. J. Pu, Q. Song, B. P. Xie, M. A. Hafiez, D. A. Chareev, A. N. Vasiliev, R. Peng, and D. L. Feng, Anomalous correlation effects and unique phase diagram of electron-doped FeSe revealed by photoemission spectroscopy, Nat. Commun. **7**, 10840 (2016).

[28] Y. Miyata, K. Nakayama, K. Sugawara, T. Sato, and T. Takahashi, High-temperature superconductivity in potassium-coated multilayer FeSe thin films, Nat. Mater. **14**, 775 (2015).

[29] J. J. Seo, B. Y. Kim, B. S. Kim, J. K. Jeong, J. M. Ok, J. S. Kim, J. D. Denlinger, S. K. Mo, C. Kim, and Y. K. Kim, Superconductivity below 20 K in heavily electron- doped surface layer of FeSe bulk crystal, Nat. Commun. **7**, 11116 (2016).

[30] P. Blaha, K. Schwarz, G. K. H. Madsen, D. Kvasnicka, and J. Luitz, *WIEN2K, An Augmented Plane Wave + Local Orbitals Program for Calculating Crystal Properties* (Karlheinz Schwarz, Techn, Universität Wien, Austria 2001).

[31] J. P. Perdew, K. Burke, and M. Ernzerhof, Generalized Gradient Approximation Made Simple, Phys. Rev. Lett. **77**, 3865 (1996).

[32] See Supplemental Material at http://link.aps.org/supplemental/10.1103/PhysRevB.95.165107 for additional electronic band structure figures of the virtual crystal doping studies discussed in the manuscript, and extra information on chalcogen substitution and nitrogen substitution for oxygen.

[33] J. Padilla and D. Vanderbilt, *Ab initio* study of $SrTiO_3$ surfaces, Surf. Sci. **418**, 64 (1998).

[34] P. T. Dumitrescu, M. Serbyn, R. T. Scalettar, and A. Vishwanath, Superconductivity and nematic fluctuations in a model of doped FeSe monolayers: Determinant quantum Monte Carlo study, Phys. Rev. B **94**, 155127 (2016).

[35] S. Zhang, J. Guan, X. Jia, B. Liu, W. Wang, F. Li, L. Wang, X. Ma, Q. Xue, J. Zhang, E. W. Plummer, X. Zhu, and J. Guo, Quantum critical transport at a continuous metal-insulator transition, Phys. Rev. B **94**, 081116 (2016).

[36] E. R. Pfeiffer and J. F. Schooley, Superconducting transition temperatures of Nb-doped $SrTiO_4$, Phys. Lett. A **29**, 589 (1969).

[37] U. Pachmayr, N. Feyn, and D. Johrendt, Structural transition and superconductivity in hydrothermally synthesized FeX (X = S, Se), Chem. Commun. **52**, 194 (2016).

[38] H. Takahashi, T. Tomita, H. Takahashi, Y. Mizuguchi, Y. Takano, S. Nakano, K. Matsubayashi, and Y. Uwatoko, High-pressure studies on T_c and crystal structure of iron chalcogenide superconductors, Sci. Technol. Adv. Mater. **13**, 054401 (2012).

[39] A. Subedi, Solvothermal density functional study of FeS, FeSe, and FeTe: Electronic structure, magnetism, phonons, and superconductivity, Phys. Rev. B **78**, 134514 (2008).

[40] K. Deguchi, Y. Takano, and Y. Mizuguchi, Physics and chemistry of layered chalcogenide superconductors, Sci. Technol. Adv. Mater. **13**, 054303 (2012).

[41] M. Hirayama, T. Misawa, T. Miyake, and M. Imada, *Ab initio* studies of magnetism in the iron chalcogenides FeTe and FeSe, J. Phys. Soc. Jpn. **84**, 093703 (2015).

[42] Y. Quan, V. Pardo, and W. E. Pickett, Formal Valence, 3*d*-Electron Occupation, and Charge-Order Transitions, Phys. Rev. Lett. **109**, 216401 (2012).

[43] W. E. Pickett, Y. Quan, and V. Pardo, Charge states of ions, and mechanisms of charge-ordering transitions, J. Phys.: Condens. Matter **26**, 274203 (2014).

[44] M. L. Kulić and O. V. Dolgov, Forward scattering peak in the electron-phonon interaction and impurity scattering of cuprate superconductors, Phys. Status Solidi b **242**, 151 (2005).